NONCONTACTING ULTRASONIC RESONANCE MEASUREMENT OF TRANSVERSE ANISOTROPY IN CYLINDERS†

Ward Johnson and G. A. Alers
Materials Reliability Division
National Institute of Standards and Technology
Boulder, CO 80303

INTRODUCTION

Ultrasonic resonance techniques using electromagnetic-acoustic transduction have been used by other authors to measure the elastic anisotropy associated with microstructural texture in plates [1-3]. The relative shift in frequency of resonant modes that would be degenerate in isotropic material provides a measure of the anisotropy. This report presents a similar resonance technique applied to a cylindrical sample, with a particular focus on the spatial filtering provided by the electromagnetic-acoustic transducer (EMAT).

A specific class of resonant modes known as "axial-shear" is employed here. In infinitely long cylinders, these modes have displacements $\mathbf{u}$ only in the axial direction $\hat{z}$ with dependence on the radial coordinate r, the azimuthal coordinate θ, and the time t [4]:

$$\mathbf{u} = \hat{z} u_o J_n(\eta r/a) \cos(n\theta - \theta_o) \cos(\omega t), \tag{1}$$

$$\eta \equiv \frac{\omega a}{v_s}, \tag{2}$$

where ω is the angular frequency, a is the radius of the rod, u_o and θ_o are constants, n is an integer, J_n is the Bessel function of the first kind of order n, and v_s is the plane-wave shear velocity. These modes are analogous to "shear-horizontal" waves propagating around the circumference of a cylinder with the wavevector in the azimuthal direction, the polarization in the axial direction, and an integral number of wavelengths, n, around the circumference.

The boundary condition of zero stress on the outer cylindrical surface is satisfied when η is such that [4]

$$n J_n(\eta) - \eta J_{n+1}(\eta) = 0. \tag{3}$$

For a given n, a, and v_s, there are an infinite number of values of η that solve Eq. (3), each value corresponding to a unique number of radial nodes of the displacement.

Review of Progress in Quantitative Nondestructive Evaluation, Vol. 14
Edited by D.O. Thompson and D.E. Chimenti, Plenum Press, New York, 1995

Only modes with $n=1$ are considered in this study. The first ten values of η that solve Eq. (3) with $n=1$ are 1.84118, 5.33144, 8.53632, 11.70600, 14.86359, 18.01553, 21.16437, 24.31133, 27.45705, and 30.60192.

Equation (1) is an exact solution of the wave equation only for infinitely long rods. The boundary conditions at the ends of finite rods cannot be satisfied by displacements of this form, and the exact solution is mathematically intractable. However, for rods with lengths much greater than the diameter, as in this study, the corresponding modes will have displacements that are almost pure shear, and Eqs. (1)-(3) will provide close approximations to the actual displacements and resonant frequencies.

EXPERIMENTAL DESIGN

Johnson, Auld, and Alers [5] presented a design for an EMAT that excites and detects torsional modes in cylindrical samples and described the associated electronics and analysis involved in measuring resonant frequencies and damping. They also presented [6] a similar design for an EMAT that couples to axial-shear modes with 24 nodes around the circumference ($n=12$). The transducer used in the present study is essentially the same as that in the latter reference, except that only two magnets are used, so that only modes with $n=1$ are excited. Figure 1 shows the EMAT design. A solenoid surrounds the cylindrical sample, and two 5.08-cm×5.08-cm×2.54-cm NdFeB magnets provide a static transverse magnetic field $\mathbf{B}$. A principal axis of the microstructural anisotropy is indicated in the figure by lines across the sample. ϕ is the angle between this axis and $\mathbf{B}$. θ is the azimuthal angle for a position $\mathbf{r}$ in a body-fixed coordinate system with θ defined to be 0 along the indicated principal axis of anisotropy. ψ is the azimuthal angular difference between $\mathbf{B}$ and $\mathbf{r}$.

The ultrasonic resonant spectrum of the coupled EMAT and sample is determined by measuring the electrical impedance across the EMAT terminals as a function of frequency with a programmable impedance analyzer [5]. In order to improve the signal-to-noise ratio, a capacitor largely eliminating the imaginary part of the impedance is placed in parallel with the EMAT. The real component of the impedance passes through a local minimum as the frequency is scanned through an ultrasonic resonance. An analysis of this circuit can be performed in a manner similar to that presented by Johnson, Auld, and Alers [5], but this will not be done here.

A solid cylindrical sample was machined from a commercial aluminum alloy rod with an Aluminum Association designation of 2024-T351. The mean finished diameter was 2.4386 ± 0.0002 cm with variations of ~ 4 μm along the length and less than 1 μm as a function of azimuthal angle. The length was 13.99 ± 0.01 cm. The sample was supported by resting one end on a flat surface (with the axis vertical), and the surrounding coil and magnets were supported on a fixture that could be rotated relative to the sample.

RESULTS

Figure 2(a) shows the real part of the measured impedance Z_{re} from 606.0 kHz to 606.9 kHz with $\mathbf{B}$ in a particular orientation relative to the sample. As described below, this orientation has $\mathbf{B}$ aligned with one of the principal axes of the anisotropy,

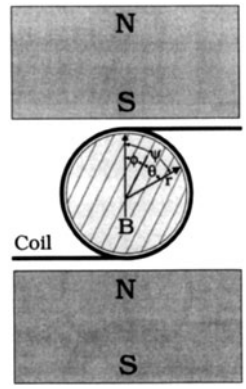

Figure 1: Schematic cross section of an EMAT that excites axial-shear modes with $n = 1$ in a cylindrical sample. "N" and "S" on the magnets indicate their polarities. A solenoid coil surrounds the sample. A principal axis of microstructural anisotropy, indicated by lines across the sample, is at an angle ϕ relative to $\mathbf{B}$. θ is the azimuthal angle between this principal axis and a position vector $\mathbf{r}$ in a body-fixed coordinate system, and ψ is the azimuthal angle between $\mathbf{r}$ and $\mathbf{B}$.

so Fig. 2(a) is labeled "$\phi = 0$". The resonant frequency of 606.761 kHz is consistent with that expected from Eq. (2) with η equal to 14.864 (the fifth solution of Eq. (3) with $n = 1$) and v_s equal to 3.124 mm/μs, as measured by Johnson, et al.,[7] in 2024 aluminum spheres.

When the EMAT is rotated 45° relative to the orientation of Fig. 2(a), the size of the inverted peak at 606.761 decreases and a second peak appears at 606.154, as shown in Fig. 2(b). An additional 45° rotation results in almost complete disappearance of the higher-frequency peak and further growth of the lower-frequency peak (Figure 2(c)).

The two peaks shown in Fig. 2 are understood to be axial-shear resonances that would be degenerate in isotropic material but are split in frequency as a result of microstructural anisotropy. Other pairs of peaks identified as axial-shear with $n = 1$ show similar behavior as the EMAT is rotated. Table 1 lists the measured resonant frequencies and corresponding theoretical values of η for the modes between 400 kHz and 900 kHz. For each pair, the two frequencies differ by approximately one part in 10^3. This splitting is more than an order of magnitude larger than that expected from the slight azimuthal variation in the sample diameter and, so, cannot be attributed to this dimensional variation. The values of v_s in the table are calculated from the measured resonant frequencies and radius using Eq. (2).

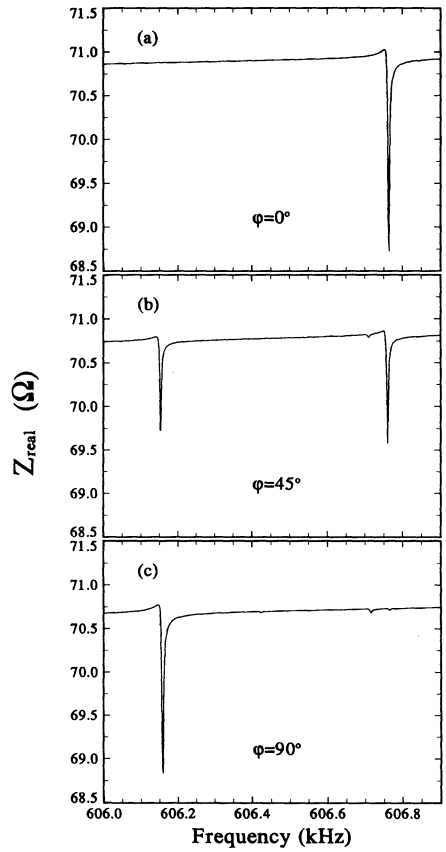

Figure 2: The real part of the impedance between 606.0 kHz and 606.9 kHz with the angle ϕ between the magnetic field and one of the principal axes of the sample anisotropy equal to 0°, 45°, and 90°.

Table 1: Resonant frequencies of the axial-shear modes with η between 11.7 and 21.2. The effective shear velocity v_s is calculated from the measured frequency and radius using Eq. 2.

η	frequency (kHz)	v_s (mm/μs)	$\Delta f/f$
11.70600	477.339/477.842	3.1240/3.1273	1.05×10^{-3}
14.86359	606.154/606.761	3.1243/3.1274	1.00×10^{-3}
18.01553	734.561/735.287	3.1237/3.1268	0.99×10^{-3}
21.16437	862.997/863.850	3.1239/3.1270	0.99×10^{-3}

For isotropic material, since θ_o in Eq. (1) is arbitrary, two orthogonal degenerate solutions with $n=1$ can be constructed with θ_o differing by $\pi/2$. Figure 3 shows the displacement patterns over a cross section for two such degenerate modes with $\eta=14.864$. For anisotropic material, the angular orientations of the normal-mode displacement patterns are no longer arbitrary, since they must be aligned with the principal axes, and, with $n=1$, θ_o is equal to 0 or $\pi/2$.

Figure 4 shows the measured amplitudes of the inverted peaks in Z_{re} at 606.154 kHz and 606.761 kHz as a function of angle ϕ. The amplitudes of the two resonances can be seen to be spatially 90° out of phase with each other.

A theoretical expression for the angular dependence of the peaks can be derived by considering that, for a continuous sinusoidal excitation of the EMAT and a given value of the damping, the vibrational amplitude u_o for a given mode is proportional to the volume integral of the product of the Lorentz body force $f(\mathbf{r})$ and the normalized displacement field for that mode (Eq. (1), omitting the time dependence):

$$u_o \sim \int f(\mathbf{r}) J_1(\eta r/a) \cos(\theta - \theta_o) dV, \tag{4}$$

for $n=1$. A proof of this relation is not presented here. Analogous relations for propagating modes in plates have been discussed by Thompson [8] and Auld [9]. The integral can be simplied for the modes of interest by noting that the electromagnetic skin depth in aluminum is only $\sim$0.1 mm at 607 kHz, so that the Lorentz force is closely approximated by a surface traction. The force is proportional to the cross product of the uniform $\mathbf{B}$ and the induced azimuthal eddy current, giving an angular dependence of $\cos\psi$. Therefore, Eq. (4) reduces to

$$u_o \sim \int_0^{2\pi} \cos(\theta - \theta_o) \cos(\psi) d\theta, \tag{5}$$

and, using the relation $\psi = \phi + \theta$ (Fig. 1), the integration yields

$$u_o \sim \cos(\phi - \theta_o). \tag{6}$$

Since the two normal modes have θ_o equal to 0 and $\pi/2$, their amplitudes are proportional to $\cos\phi$ and $\sin\phi$, respectively. The transduction involved in the detection of resonant vibrations is essentially the reverse of that involved in the excitation, so the amplitude of currents induced in the EMAT coils for a given vibrational amplitude will have the same angular dependence as u_o, and the magnitude of the resonance peak measured with the impedance analyzer, which is

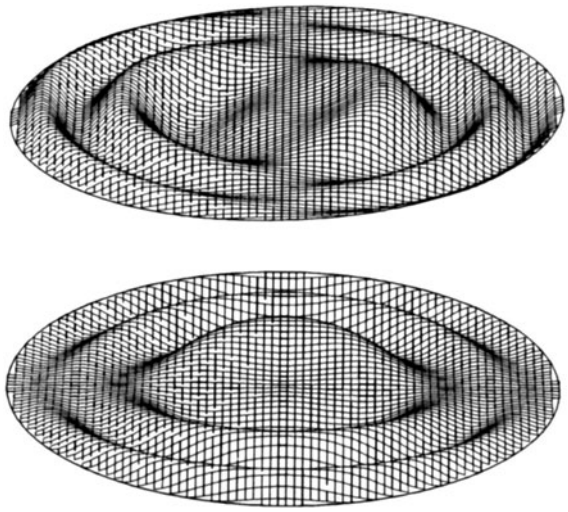

Figure 3: Amplitudes of axial-shear displacements over the cross section of a cylinder for $n=1$, $\eta = 14.864$.

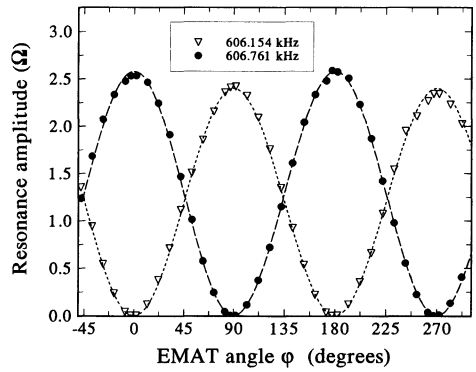

Figure 4: The measured amplitudes (ohms) of the inverted peaks in Z_{re} at 606.154 kHz and 606.761 kHz as a function of angle ϕ.

dependent on the product of the excitation and detection efficiencies, will be proportional to $\cos^2\phi$ or $\sin^2\phi$. The dashed curves in Fig. 4 show this theoretical dependence with the overall magnitude scaled to approximately match the data. The measured angular dependence is in good agreement with the theory.

CONCLUSION

In addition to describing a technique for measuring the frequency splitting resulting from anisotropy in solid cylinders, this report provides a demonstration of the nearly complete spatial filtering that is attainable with EMATs. The spatial filtering makes resonant spectra relatively easy to interpret and provides information on the symmetry of the resonant modes and the related sample microstructure. The modes used here, with $n=1$, measure only the first moment of the anisotropy. Modes with higher values of n could be used to measure higher-order moments.

Since this noncontacting transduction technique results in negligible external damping of the resonant vibrations, the measured peak widths approach their intrinsic values, and a frequency splitting much smaller than that reported here could be resolved. In aluminum alloys, the resonant peak widths at half maximum are only about 6 Hz for the resonances near 606 kHz (see Fig. 2 and Ref. 5), so that an anisotropy on the order of 1 part in 10^5 could be measured.

REFERENCES

1. Zh. G. Nikiforenko, N. A. Glukhov, and I. I. Averbukh, Sov. J. Nondestructive Testing, **4**, 427 (1971).
2. K. Kawashima, J. Acoust. Soc. Am. **87**, 681 (1990).
3. A. V. Clark, C. M. Fortunko, M. G. Lozev, S. R. Schaps, and M. C. Renken, Research in Nondestructive Evaluation, **4**, 165 (1992).
4. A. C. Eringen, and E. S. Şuhubi, *Elastodynamics, Vol. II* (Academic, New York, 1975).
5. W. Johnson, B. A. Auld, and G. A. Alers, J. Acoust. Soc. Am., **95**, 1413 (1994).
6. W. Johnson, B. A. Auld, and G. A. Alers , *Review of Progress in Quantitative Nondestructive Evaluation, Vol. 13B*, eds. D. O. Thompson and D. E. Chimenti (Plenum, New York, 1994), p. 1603.
7. W. L. Johnson, S. J. Norton, F. Bendec, and R. Pless, J. Acoust. Soc. Am., **91**, 2637 (1992).
8. R. B. Thompson, IEEE Transactions on Sonics and Ultrasonics, **SU-25**, 7 (1978).
9. B. A. Auld, *Acoustic Waves and Fields in Solids, Vol. II* (John Wiley and Sons, New York, 1973), pp. 155-162.